Structural and magnetic properties of the intergranular amorphous phase in FeNbB nanocrystalline alloys

2000 J. Phys.: Condens. Matter 12 9085

(http://iopscience.iop.org/0953-8984/12/42/313)

J. Phys.: Condens. Matter **12** (2000) 9085–9093. Printed in the UK PII: S0953-8984(00)11845-4

Structural and magnetic properties of the intergranular amorphous phase in FeNbB nanocrystalline alloys

I Škorvánek†, J Kováč† and J-M Grenèche‡

† Institute of Experimental Physics, Slovak Academy of Sciences, Watsonova 47, 043 53 Košice, Slovakia

‡ Laboratoire de Physique de l'Etat Condensé, UPRESA CNRS 6087, Université du Maine, Faculté des Sciences, 72085 Le Mans Cedex 9, France

Received 14 February 2000, in final form 6 September 2000

Abstract. Static and hyperfine magnetic characteristics of an $Fe_{80.5}Nb_7B_{12.5}$ nanocrystalline alloy consisting of bcc-Fe nanograins embedded in residual amorphous matrix are compared to those of a hypothetical composite alloy which consists of bulk bcc-Fe and an amorphous alloy in the as-quenched state. The chemical composition of the latter and the proportions of these two constituents were estimated from the mass balance considerations according to the experimentally determined crystalline fraction. The two-phase description of such a hypothetical composite alloy is *a posteriori* confirmed by the low temperature magnetic characteristics. The degree of compositional heterogeneity of the residual amorphous matrix in the nanocrystalline sample is found to be considerably higher as compared to that of its bulk single-phase as-quenched counterpart. The differences of magnetic behaviour versus temperature allow some aspects of the chemical and structural nature of the intergranular amorphous phase in nanocrystalline alloy to be discussed.

1. Introduction

Soft magnetic Fe-based nanocrystalline alloys, which are produced by partial devitrification of melt-spun amorphous precursors, exhibit a duplex structure with a nanocrystalline dispersion of bcc-Fe grains embedded within a residual amorphous matrix with higher crystallization temperature. In addition to the intrinsic values of magnetic parameters in the constituent phases, a significant role in determining the magnetic behaviour of nanocrystalline systems is played also by the effects of reduced dimensionality. Among the relevant parameters which govern this magnetic behaviour are: (i) the volume fraction of the crystalline phase, (ii) the size of the crystalline grains and (iii) the nature of the intergranular phase.

The crystalline content can be controlled by both annealing time and appropriate annealing temperature. The number of crystalline grains and their size are dependent on the atomic composition of the amorphous precursor and the relative diffusivities of the different constituents [1, 2]. In the course of annealing, especially in the temperature range where the growth of the bcc-Fe nanocrystals occurs, the intergranular amorphous matrix is subjected to substantial microstructural and chemical changes due to its enrichment in elements which are expelled from bcc-Fe precipitates [3]. The local microstructural changes are closely correlated with the corresponding changes in magnetic properties. Therefore, the nature of residual amorphous matrix and its properties should be different in comparison to the single-phase melt-spun amorphous material.

0953-8984/00/429085+09$30.00

It has been reported for several nanocrystalline alloy systems that after devitrification the increase in T_c(am) of residual matrix takes place with respect to the value expected from the known compositional dependence for the bulk amorphous materials [4–9]. The non-homogeneity of the amorphous phase arising from the diffusion during nanocrystallization [4, 5] and the penetration of the exchange field caused by the nanocrystallites into the residual amorphous matrix [6] have been suggested as an origin of this behaviour. The later mechanism, originally suggested by Hernando *et al* in nanocrystalline FeNbBCu-type alloys [6], was reported to be operative also in some other Fe-based nanocrystalline systems [7–9]. A model based on an exponential decay of the exchange penetration from Fe crystallites into the remaining amorphous phase has shown a good quantitative agreement between calculated and measured values of T_c(am) for FeZrB-type alloys [7].

In this paper, we present some relevant magnetic characteristics obtained on both melt-spun amorphous $Fe_{80.5}Nb_7B_{12.5}$ alloy and nanocrystalline $Fe_{80.5}Nb_7B_{12.5}$ alloy, which was isothermally heat treated for 1 hour at 510 °C leading to partial crystallization. These results were obtained by static magnetic measurements and ^{57}Fe Mössbauer spectrometry, which offer data averaged over the different constituents and local insight at each ^{57}Fe nucleus probe, respectively. Using simple mass balance considerations we have estimated the average composition of the residual amorphous matrix. Finally, an additional single-phase amorphous ribbon having the same chemical composition was prepared by the melt-spinning technique in order to compare its magnetic and hyperfine properties to those of the residual amorphous matrix in the heat treated nanocrystalline alloy.

2. Experiment

Amorphous ribbons of $Fe_{80.5}Nb_7B_{12.5}$ alloy were prepared by the method of planar flow casting. Pieces of these ribbons were annealed under protective argon atmosphere for 1 hour at temperature 510 °C in order to prepare the nanocrystalline samples for magnetic and Mössbauer characterization. The above heat treatment resulted in the formation of about 26% bcc-Fe phase in the investigated alloy [10]. From transmission electron microscopy (TEM) observations and from the small angle neutron scattering (SANS) experiments [11], the size of the crystalline bcc-Fe grain is estimated at 10–13 nm. If one assumes that due to their very poor solubility only negligible numbers of Nb and B atoms are dissolved in bcc-Fe nanocrystalline grains, then the average composition of residual amorphous matrix phase can be estimated by using the following mass balance equation:

$$Fe_{80.5}Nb_7B_{12.5} \rightarrow 0.26\ Fe + 0.74\ Fe_{73.6}Nb_{9.5}B_{16.9}.$$

In view of this result we have prepared the new melt-spun amorphous ribbon with a nominal composition $Fe_{73.5}Nb_{9.5}B_{17}$ that was used in our work for the sake of comparative study of magnetic and hyperfine properties.

Measurements of the saturation magnetization in investigated samples have been performed by using a vibrating sample magnetometer (VSM) over the temperature range from 4.2 K to 800 K. The value of magnetic field applied during measurement was 0.4 T.

^{57}Fe Mössbauer experiments were performed in transmission geometry using a conventional spectrometer with a constant acceleration signal and a ^{57}Co source diffused into a rhodium matrix. The samples were located under vacuum either in a bath cryostat or a cryofurnace to carry out spectra at temperatures comprised between 4.2 and 800 K. 77 or 300 K Mössbauer spectra were systematically collected after high-temperature measurements to check the occurrence of any further structural transformation. Samples were maintained perpendicular to the unpolarized γ-beam to get Mössbauer spectra but some texture free spectra

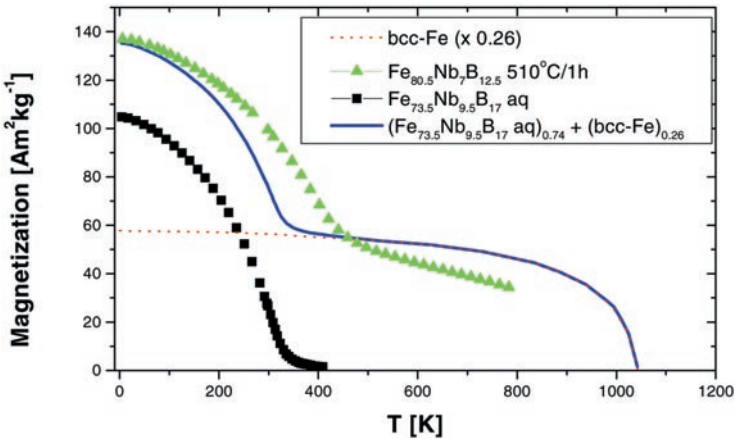

Figure 1. Magnetization curves of as-quenched amorphous $Fe_{73.5}Nb_{9.5}B_{17}$ and the nanocrystalline $Fe_{80.5}Nb_7B_{12.5}$ alloy annealed at 510 °C for 1 hour and that expected for the hypothetical composite material {0.26 bcc-Fe(bulk) + 0.74 $Fe_{73.5}Nb_{9.5}B_{17}$(as-q)}.

were also obtained using the magic angle configuration to check the effect of the ferromagnetic domain texture.

Mössbauer spectra were analysed using specific fitting procedures with the Mosfit program. In the case of amorphous alloys, the description only consists in a discrete distribution of hyperfine field or of quadrupolar splitting linearly correlated with that of isomer shift, below and above the Curie point of the as-quenched amorphous ribbon, respectively. In other respects, the spectra of nanocrystalline samples are analysed by considering three main components: (i) the sextet with sharp lines attributed to the crystalline grains; (ii) the contribution with broad lines located in the internal wings of external lines of previous component assigned to the intermediate zone; (iii) the broad line sextet at low temperature, which progressively collapses to a broad line central quadrupolar doublet at high temperatures due to the intergranular phase. The first component was described using a single sextet with parameters free during the fitting procedure, the second one with a discrete distribution of hyperfine fields, while the latter one resulted from either a discrete distribution of hyperfine field or quadrupolar splitting linearly correlated to that of isomer shift. Details of the refinement procedure were previously reported in [12].

3. Results and discussion

The temperature dependences of magnetization for the as-quenched amorphous $Fe_{73.5}Nb_{9.5}B_{17}$ and the heat treated nanocrystalline $Fe_{80.5}Nb_7B_{12.5}$ samples are shown in figure 1. The latter is compared to that expected for the hypothetical composite material {0.26 bcc-Fe(bulk) + 0.74 $Fe_{73.5}Nb_{9.5}B_{17}$(as-q)}. Such a model magnetization curve results from the linear combination of independent magnetizations. Three features can be clearly observed: (i) an excellent agreement can be seen only at 0 K; (ii) below 450 K, the experimental magnetization remains higher than the total model one and (iii) it becomes smaller at higher temperatures.

Figure 2 shows the derivatives of the magnetization curves, dM/dT, in the temperature range where the bulk amorphous $Fe_{73.5}Nb_{9.5}B_{17}$ and $Fe_{80.5}Nb_7B_{12.5}$ samples and the intergranular amorphous phase of the nanocrystalline $Fe_{80.5}Nb_7B_{12.5}$ sample exhibit a transition

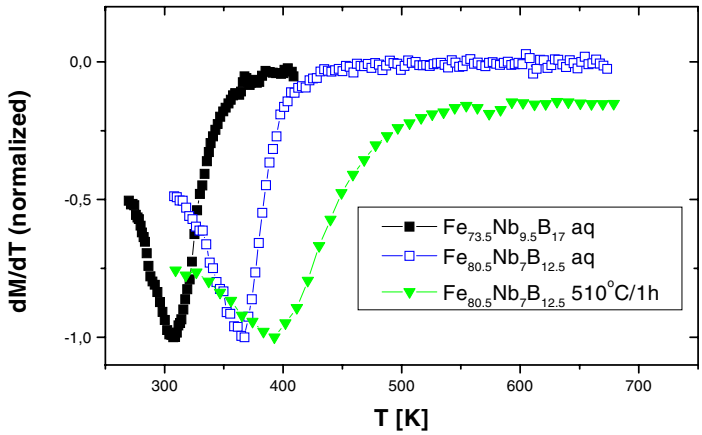

Figure 2. Derivatives of the magnetization curves for amorphous $Fe_{73.5}Nb_{9.5}B_{17}$ and $Fe_{80.5}Nb_7B_{12.5}$ in the as-quenched state and for the nanocrystalline $Fe_{80.5}Nb_7B_{12.5}$ sample annealed at 510 °C/1 h.

from the ferromagnetic to paramagnetic state. The values of Curie temperature for both as-quenched amorphous samples are well defined as can be seen from sharp minima in corresponding dM/dT peaks. The remarkably broader peak in dM/dT for the nanocrystalline sample clearly indicates an inhomogeneous nature of the residual amorphous phase, which results in smearing out of the local Curie temperature.

A series of Mössbauer spectra recorded at different temperatures on the as-quenched amorphous $Fe_{73.5}Nb_{9.5}B_{17}$ sample are plotted in figure 3. The hyperfine structure turns rapidly from a broad line magnetic sextet into a broad line quadrupolar doublet, as usually observed. The same evolution is noticed for the $Fe_{80.5}Nb_7B_{12.5}$ sample in the as-quenched state. Figure 4 illustrates a selection of Mössbauer spectra of the nanocrystalline $Fe_{80.5}Nb_7B_{12.5}$ sample annealed at 510 °C for 1 h. One clearly observes the sharp line sextet attributed to the crystalline grains and the broad line magnetic feature that progressively collapses to an asymmetrical quadrupolar doublet at high temperature. It is important to note that this second component occurs as magnetically ordered even above the Curie temperature of the amorphous phase. The set of spectra was modelled on the basis of three components, according to the fitting procedure described in [12].

Figure 5 compares the temperature dependences of the mean hyperfine field at iron nuclei estimated by Mössbauer spectrometry on amorphous $Fe_{73.5}Nb_{9.5}B_{17}$ and $Fe_{80.5}Nb_7B_{12.5}$ in the as-quenched state and on the intergranular amorphous remainder of the nanocrystalline $Fe_{80.5}Nb_7B_{12.5}$ sample. The as-quenched phases display sharp and well defined magnetic transitions (the highest T_c corresponds to the largest iron content alloy) while the mean hyperfine field of the amorphous remainder of the nanocrystalline alloy progressively vanishes with increasing temperature but differs significantly from zero at high temperatures. In addition, the nice agreement observed at 0 K is consistent with the first feature mentioned above for the magnetization data: both clearly indicate that the mean chemical composition of the amorphous remainder is close to that of $Fe_{73.5}Nb_{9.5}B_{17}$ alloy.

In addition, to obtain a local insight into the atomic structural heterogeneity, the hyperfine field distributions of the as-quenched $Fe_{73.5}Nb_{9.5}B_{17}$ alloy are then compared in figure 6 to those characteristic of the amorphous remainder of the nanocrystalline $Fe_{80.5}Nb_7B_{12.5}$ sample. At rather low temperatures, the disagreement is not so pronounced, confirming the previous

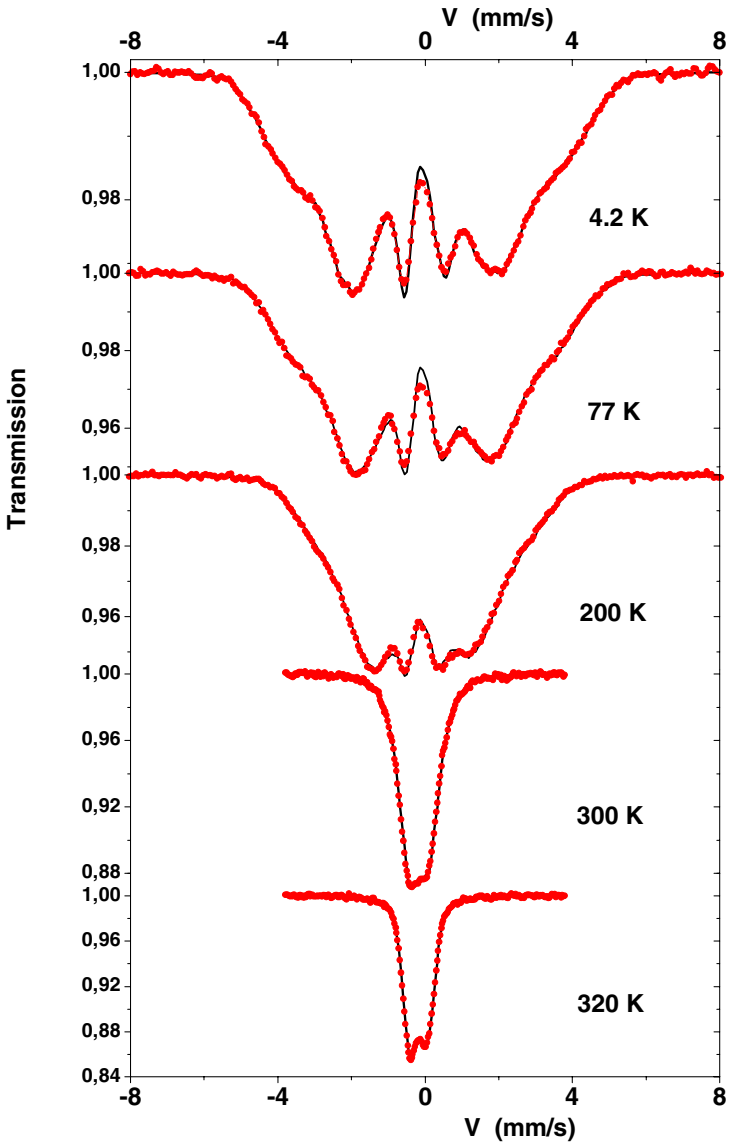

Figure 3. Mössbauer spectra recorded at given temperatures on the as-quenched amorphous $Fe_{73.5}Nb_{9.5}B_{17}$ sample.

conclusion, but it significantly increases with increasing temperature. At any temperature, the $P(B)$ distributions which correspond to amorphous residual phase are distinctly broader than those of melt-spun amorphous alloy. Above the Curie point of the amorphous phase, one observes a high field contribution in addition to a low field prevailing peak that can be considered as resulting from paramagnetic iron sites. Those results are consistent with those mentioned in the previous section.

All these features have to be explained in terms of either penetration field resulting from the coupling between nanocrystalline grains, and/or the chemical heterogeneity of the amorphous remainder.

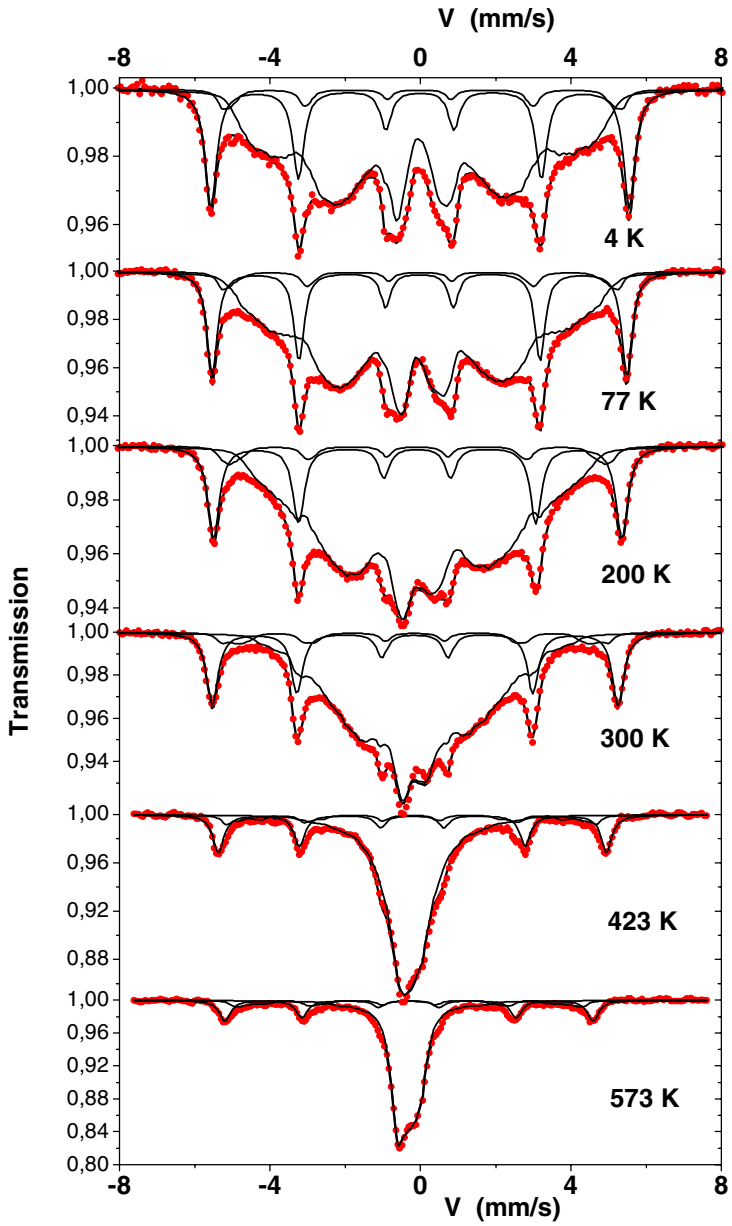

Figure 4. Mössbauer spectra recorded at given temperatures of the nanocrystalline $Fe_{80.5}Nb_7B_{12.5}$ sample annealed at 510 °C/1 h. Subspectra are also reported (see text).

As seen in figure 2, the Nb and B enrichment in the bulk as-quenched $Fe_{73.5}Nb_{9.5}B_{17}$ ribbon as compared to the as-quenched $Fe_{80.5}Nb_7B_{12.5}$ alloy results in a marked decrease of Curie temperature. However, the opposite behaviour is observed for the similarly Nb and B enriched amorphous remainder in the nanocrystalline $Fe_{80.5}Nb_7B_{12.5}$ alloy. Therefore, the observed increase in T_c for the latest sample seems to be associated with the penetration of exchange field from nanocrystalline grains, which overtrumps the expected decrease of Curie temperature due to compositional changes.

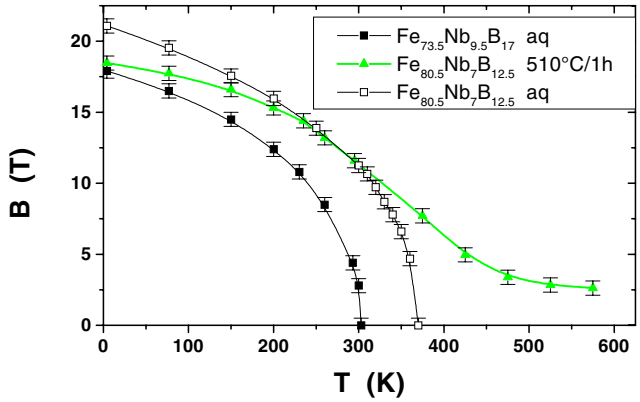

Figure 5. Temperature dependences of both the mean hyperfine field of amorphous $Fe_{73.5}Nb_{9.5}B_{17}$ and $Fe_{80.5}Nb_7B_{12.5}$ in the as-quenched state and of the intergranular amorphous remainder of the nanocrystalline $Fe_{80.5}Nb_7B_{12.5}$ sample.

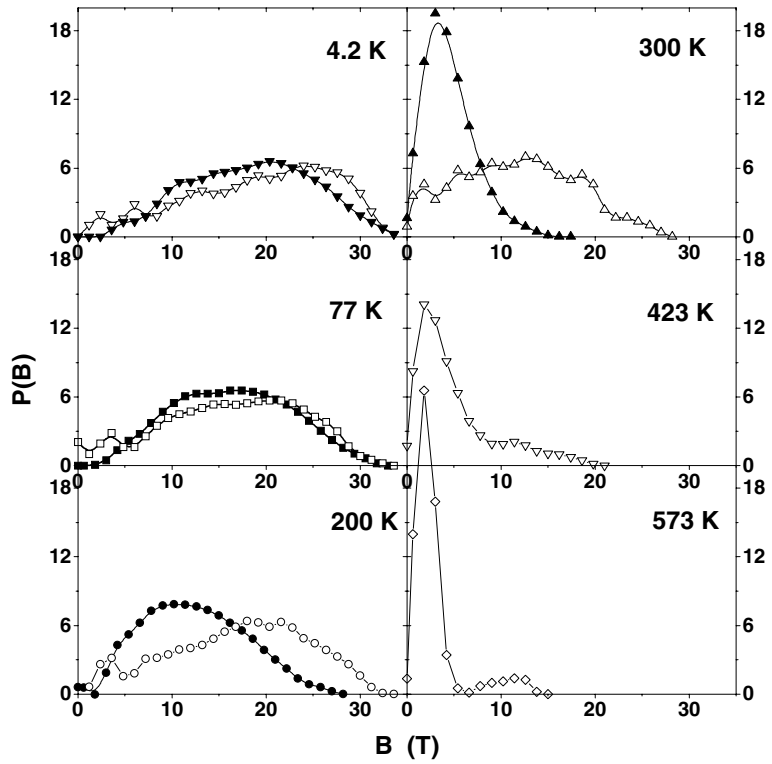

Figure 6. Hyperfine field distributions of the as-quenched $Fe_{73.5}Nb_{9.5}B_{17}$ alloy (solid symbols) compared to those characteristic of the intergranular amorphous remainder of the nanocrystalline $Fe_{80.5}Nb_7B_{12.5}$ sample (open symbols) at given temperatures (note the scales).

The primary crystallization of bcc-Fe is essentially controlled by diffusion processes, and, therefore, it is accompanied by changes of the chemical composition in the environment of growing crystallites. The growth of crystallites is hindered by slowly diffusing inhibitors

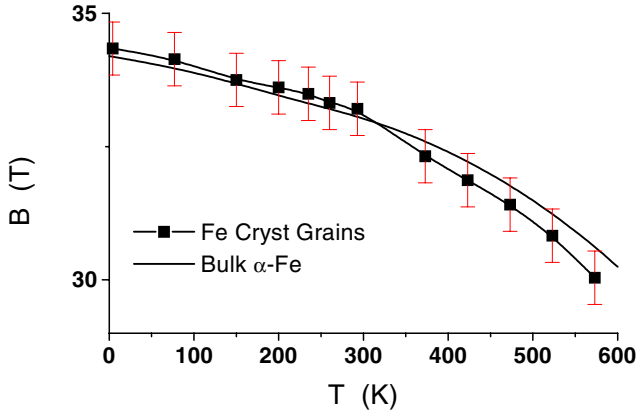

Figure 7. Evolution versus temperature of the hyperfine field corresponding to the crystalline grains compared to that of bulk α-Fe.

accumulating at the surface of the crystallite [13]. In the case of the present alloy, it is primarily the Nb enrichment which leads to a diffusion barrier stopping the growth of crystallites. The extremely high field values of the amorphous remainder, which occur even at 300 K, are close to those observed usually in some FeB amorphous alloys, so they have to be attributed to Fe atoms preferentially surrounded by Fe, which are located outside Nb-enriched zones. In another respect the low field values suggest the existence of Nb-rich zones: these iron atoms have to be located in close contact with the Nb-rich shells created around the crystallites during the crystallization process. Such a situation was recently modelled during the devitrification of Finemet alloys [14]. Such features totally confirm the strong heterogeneity of the amorphous remainder. It is also consistent with the progressive vanishing of the mean hyperfine field value with increasing temperature, as observed in figure 3.

The temperature dependency of the hyperfine field of the crystalline grains well agrees with that of bcc-Fe bulk phase for temperatures below the Curie point but tends to be smaller above T_c as illustrated in figure 7. Moreover, from figure 1 it follows that at temperatures higher than 450 K also the magnetization values of the nanocrystalline sample decrease more rapidly than those of the bcc-Fe bulk sample. Such behaviours indicate that with an increase of measuring temperature well above the Curie temperature of the intergranular amorphous remainder certain nanocrystalline grains could behave as an assembly of weakly interacting single domain particles dominated by the thermal fluctuations, as expected for the present volumetric crystalline fraction [15]. It has been shown that in such a case the small sizes of crystalline grains favour the presence of superparamagnetic effects [16, 17]. With a sufficient increase of measuring temperature the distance between some grains became higher than the critical one required for complete domination of thermal fluctuations by the magnetic coupling between crystalline grains, and, therefore, the effects of thermal fluctuations can play a noticeable role in determining the overall magnetic behaviour of the investigated material above the Curie temperature of the intergranular matrix. The presence of very small grains in the corresponding distribution of particle sizes as observed by SANS [11] may support such an explanation. Nevertheless, within this high temperature range the hyperfine field values at iron sites located in the intergranular phase remain unusually large and cannot be only explained on the basis of the atomic structure of the intergranular phase. One has also to consider the presence of the penetrating contribution of exchange fields originating from

interacting magnetic crystallites. Additional studies of the above effects by using the series of nanocrystalline $Fe_{80.5}Nb_7B_{12.5}$ samples with different volume fractions of crystalline phase are currently in progress.

4. Conclusions

In this paper, both the magnetization and the mean hyperfine field of the intergranular amorphous phase in the FeNbB nanocrystalline alloy were compared to those of an analogous amorphous alloy in as-quenched state. The average chemical composition of the corresponding residual amorphous phase has been estimated from mass balance consideration taking into account the volume fraction of the formed bcc-Fe nanograins in partially crystallized parent amorphous precursor. Striking differences in temperature dependences of investigated magnetic and hyperfine parameters were observed for the intergranular amorphous phase and its single phase melt-spun analogue. These differences start to be more and more remarkable at temperatures close to the Curie point of the amorphous phase, while a relatively good agreement between the investigated characteristics has been found at low temperature. The results observed using the present approach confirm the strong chemical heterogeneity of the intergranular phase in the FeNbB nanocrystalline alloys and support clearly the contribution of penetrating fields caused by the nanocrystalline grains at high temperatures, both in agreement with previous works.

Acknowledgments

The authors would like to thank Dr P Duhaj and Dr P Švec for providing the amorphous $Fe_{80.5}Nb_7B_{12.5}$ ribbon. This work was supported by the France–Slovak (CNRS–SAS) exchange program. IŠ and JK acknowledge the support of the Volkswagen Foundation under project No VW-I/75961 and VEGA under project No 2/5141.

References

[1] Köster U, Schunemann U, Blank-Bewesdorff M, Brauer S, Sutton M and Stephenson G B 1991 *Mater. Sci. Eng.* A **133** 611
[2] Mat'ko I, Duhaj P, Švec P and Janičkovič D 1994 *Mater. Sci. Eng.* A **179/180** 557
[3] Inoue A, Takeuchi A, Makino A and Masumoto T 1996 *Sci. Rep. RITU* A **42** 143
[4] Yavari R 1995 *Nanostructured and Non-Crystalline Materials* ed M Vazquez and Hernando (Singapore: World Scientific) p 35
[5] Suzuki K, Cadogan J M, Sahajwalla V, Inoue A and Masumoto T 1997 *Mater. Sci. Eng.* A **226–228** 554
[6] Hernando A, Navaro I and Goria P 1995 *Phys. Rev.* B **51** 3281
[7] Garitaonandia J S, Schmool D S and Barandiaran J M 1998 *Phys. Rev.* B **58** 12, 147
[8] Suzuki K and Cadogan J M 1998 *Phil. Mag. Lett.* **77** 371
[9] Khalladi A, Tong Z, Surinach S, Tonejc A M, Tonejc A and Baró M D 1999 *Mater. Sci. Forum* **307** 95
[10] Škorvánek I, Kováč J, Marcin J, Duhaj P and Gerling R 1999 *J. Magn. Magn. Mater.* **203** 226
[11] Marcin J, Wiedenmann A and Škorvánek I 2000 *Physica* B **276–278** 870
[12] Miglierini M and Grenèche J M 1997 *J. Phys.: Condens. Matter* **9** 2303
Miglierini M and Grenèche J M 1997 *J. Phys.: Condens. Matter* **9** 2321
[13] Zhang Y, Hono K, Inoue A, Makino A and Sakurai T 1996 *Acta Mater.* **44** 1497
[14] Borrego J M, Conde C F, Conde A, Peña-Rodríguez V A and Grenèche J M 2000 *J. Phys.: Condens. Matter* **12** 8089
[15] Grenèche J M, Miglierini M and Slawska-Waniewska A 2000 *Hyperfine Interact.* **126** 27
[16] Slawska-Waniewska A, Gutowski M, Lachowicz H K, Kulik T and Matyja H 1992 *Phys. Rev.* B **46** 14, 594
[17] Škorvánek I and O'Handley R C 1995 *J. Magn. Magn. Mater.* **140–144** 467